DEVELOPING NEW METRICS FOR COMPARISON OF DIFFUSION PROPAGATORS

Luis Miguel Lacerda[1], Jonathan I. Sperl[2], Gareth Barker[1], and Flavio Dell'Acqua[1]

[1]*Centre for Neuroimaging Sciences, Institute of Psychiatry, King's College London, London, Denmark Hill, United Kingdom,* [2]*GE Global Research, Munich, BY, Germany*

TARGET AUDIENCE - This abstract is targeted for researchers developing new methods for diffusion imaging.

PURPOSE – One of the advantages of Diffusion Spectrum Imaging (DSI) is the ability to recover an approximate description of the actual diffusion propagator at the expense, however, of very long acquisition times [1]. New methods like compressed sensing (CS) have been proposed to overcome some of these limitations [2, 3] but are often compared with the non-accelerated version without a proper direct exploration of the differences from the true underlying diffusion propagator. A standard approach to evaluate the performance of CS and other acceleration methods is to compare the reconstructed orientation distribution functions (ODFs) against a predefined "gold standard". Although ODF profiles provide useful information, other measures need to be considered to better characterize all the information available in the diffusion propagator [4] and better compare performance across different reconstruction methods. In this study we will explore how this information can be summarized using a range of metrics, in order to evaluate of how much information we preserve from the ideal propagator when using both standard acquisition methodologies and new acceleration methods like compressed sensing. The specific metrics we evaluate are the return to origin probability (P0), the mean square displacement (MSD) [5] and an angular complexity index (ACI) defined similarly to a General Fractional Anisotropy estimated for increasing radii of the propagator ($ACI\ (r) = std(Propagator(r))/rms(Propagator(r))$).

METHODS – A crossing fibre configuration of 70° was simulated as the sum of two tensors with a diffusivity profile of [1.7 0.2 0.2] x10^{-3} mm^2/s (no diffusional exchange). Additionally, a single fibre ([1.7 0.2 0.2] x10^{-3} mm^2/s) and an isotropic component ([0.7 0.7 0.7] x10^{-3} mm^2/s) were also simulated. For each configuration datasets from different acquisition schemes were simulated: an "ideal" DSI acquisition defined over a 125x125x125 Cartesian grid with a maximum b-value of 260000 s/mm^2, a high resolution DSI acquisition with b-value of 8000 s/mm^2 and 11x11x11 grid yielding 515 sampling points and a medium resolution DSI acquisition with a max b-value of 4000 s/mm^2 with 7x7x7 and 123 sampling points. For the last two acquisition schemes two corresponding CS schemes were also generated with an acceleration factor of R=4 as described in previous studies [2] and with 129 and 30 points, respectively. All data were simulated without noise. For each dataset the propagator was estimated using either the standard DSI or the corresponding CS reconstruction. ODF profiles, P0, MSD and ACI metrics where then calculated.

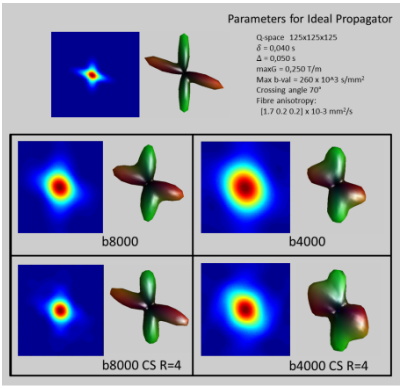

Fig 1 – Visual comparison of different propagators and associated ODFs from distinct simulated datasets at 70° crossing.

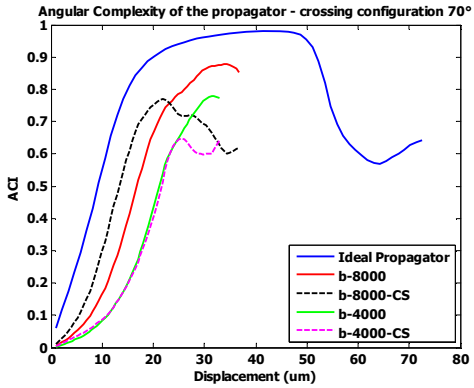

Fig 2 – Different Angular complexity profiles quantified by the ACI over the displacement radius for the different simulated datasets.

	Single Fibre	
	P0	MSD
b8000	1.283	0.001
b4000	5.399	0.002
b8000_CS_R4	1.157	0.316
b4000_CS_R4	6.821	0.045

	Isotropic	
	P0	MSD
b8000	0.138	0.000
b4000	0.715	0.002
b8000_CS_R4	0.539	0.795
b4000_CS_R4	0.849	0.354

	Crossing	
	P0	MSD
b8000	1.281	0.006
b4000	5.376	0.003
b8000_CS_R4	1.401	0.562
b4000_CS_R4	9.220	0.338

Table 1 – NMSE between the ideal propagator and the distinct simulated datasets propagator for different microstructure configurations.

RESULTS AND DISCUSSION – Figure 1 depicts the propagator and associated ODF for different simulated acquisitions in the case of a 70° crossing. Differences in the ODF profiles as well as in the propagator compared to the ideal case are evident for all four acquisition schemes. As expected, the propagator and ODF with both fully-acquired scheme show a decreasing angular resolution as the b-value and number of points are reduced. CS reconstructed ODFs also present some instabilities in their reconstruction, however, in the case of the high resolution dataset, it seems that the CS reconstruction is better at preserving angular resolution than the non-accelerated reconstruction. Figure 2 shows the angular complexity profiles of the different simulated datasets, again in the case of a crossing fibre configuration. By analyzing the different profiles we can distinguish specific behaviors depending on displacement, and can identify degradation of information from the ideal propagator with decreasing b-value. In particular, we observe that in high resolution DSI acquisitions and for shorter displacements, CS presents a sharper profile when compared with standard (unaccelerated) acquisitions (this is consistent with the fact that the CS adopted in this study does not use Hanning windowing in its implementation). However, for larger displacement, the CS reconstruction shows a decreasing complexity compared to the full acquisition likely due to the presence of numerical instabilities in the propagator background. For the medium resolution acquisition, CS and full sampling show similar complexity for low displacement values but again a decrease in complexity is seen in the CS for larger displacements. It is important, though, to remember the great reduction of data points between the classical acquisitions and their CS counterparts. Finally, Table 1 summarizes, for different fibre configurations, results of the normalized mean squared error (NMSE) between each simulated technique and the ideal propagator of the PO and MSD. The values shown in this table show that standard acquisition methods appear to retain more information when compared to CS reconstructions, presenting lower NMSE values. More tests are required to validate these results for a greater range of configurations and sampling schemes, however.

CONCLUSION - In this work we have presented preliminary results that may allow a more robust analysis and comparison of diffusion data and different acceleration methods. Indices like P0, MSD and ACI appear to be helpful in characterizing different features of the diffusion propagator and add complementary information to the ODF when comparing different reconstruction methods. Future works will extend this analysis to include a full set of 1D, 2D and 3D descriptors of the spatial information available in a single propagator and across large regions (multi-voxel). The final aim is to develop and use this framework to compare different methods to recover diffusion propagators including compressed sensing, non-Cartesian sampling methods, denoising and undersampling techniques based on sparse dictionaries [6, 7, 8].

[1] Wedeen, V. J. et al, MRM 2005, 54(6), 1377–86; [2] Menzel, M. I. et al MRM 2011, 66(5), 1226–33; [3] Landman, B. et al, ISMRM 2010; [4] Özarslan, E. et al, NeuroImage, 78, 16–32; [5] Assaf, Y. et al, MRM 2000, 43(2), 191–9; [6] Gramfort, A et al, Medical Image Analysis 2013 18(1), 36-49; [7] Merlet, S. et al, Medical Image Analysis 2013 17(7), 830-43; [8] Descoteaux, M. et al (2011) Medical image analysis, 15(4), 603–21.